Colloid Polym Sci 276:968–975 (1998)

ORIGINAL CONTRIBUTION

C.A.P. Joziasse
D.W. Grijpma
J.E. Bergsma
F.W. Cordewener
R.R.M. Bos
A.J. Pennings

The influence of morphology on the (hydrolytic degradation of as-polymerized and hot-drawn poly(L-lactide))

Received: 10 February 1998
Accepted: 15 May 1998

C.A.P. Joziasse · D.W. Grijpma
A.J. Pennings (✉)
Department of Polymer Chemistry
University of Groningen
Nijenborgh 4
9747 AG Groningen
The Netherlands

J.E. Bergsma · F.W. Cordewener
R.R.M. Bos
Department od Oral
and Maxillofacial Surgery
University Hospital Groningen
P.O. Box 30001
9700 RB Groningen
The Netherlands

Abstract The influence of morphology on the hydrolytic degradation behavior of poly(L-lactide) has been studied. High molecular weight and highly crystalline as-polymerized poly(L-lactide) was obtained in high yields through melt polymerization. Poly(L-lactide) fiber with a draw ratio of 5.6 was obtained by hot-drawing solution-spun fiber.

During the bulk degradation of as-polymerized poly(L-lactide), a rapid decrease of molecular weight and tensile properties was observed. This could be explained by the morphology of the material and the presence of thermal stresses and subsequent generation of micro-cracks. The lamellar crystallites in as-polymerized poly(L-lactide) appeared to be very stable towards hydrolysis. The resorption time of high molecular weight as-polymerized poly(L-lactide) in vivo was estimated at 40–50 yr by extrapolation of molecular weight data.

Hot-drawn poly(L-lactide) fiber showed exceptional hydrolytic stability under a static load and substantially retained its mechanical properties over a period of more than 5 yr. The high perfection of the crystalline fiber and the elimination of micro-voids obtained by hot-drawing prevented penetration of water and induced surface erosion of the fiber.

Key words poly(L-lactide) – hydrolytic degradation – morphology – crystallinity – hot-drawn

Introduction

Over the past two decades bioresorbable poly(lactide)s have been studied extensively for their biomedical applications [1–11] and fracture fixation devices for the oral and maxillofacial areas have been successfully applied in our University [6–11]. To mimic as closely as possible the mechanical properties of stainless steel and titanium, initially we focused on high strength high modulus materials. High molecular weight and highly crystalline as-polymerized poly(L-lactide) (as-pol. PLLA or PLA100) showed excellent tensile and impact properties [12]. Furthermore, promising clinical results in mandibular and zygomatic fracture fixation and in the repair of the orbital floor were reported for as-pol. PLA100 [10, 11, 13]. From good correlation between preliminary in vivo and in vitro degradation data [5] as-pol. PLA100 was estimated to resorb in 3–4 yr. However, clinical follow-up after three years of patients treated for a zygomatic fracture [14, 15] revealed that highly crystalline remnants of as-pol. PLA100 were still present.

Poly(lactide)s degrade by hydrolytic bulk degradation, i.e. water penetrates the sample after which random hydrolytic scission of the polymer chains occurs throughout the specimen. The in vivo and in vitro degradation of poly(lactide)s is influenced by a number of intrinsic and extrinsic factors, such as molecular weight, (stereo)

copolymer composition, the presence of monomer and catalyst residues [16] and the degradation medium and temperature. Other biodegradable materials, such as poly(anhydride)s [17] and poly(ortho ester)s [18] have been reported to degrade by surface erosion, instead of bulk degradation. In this case, hydrolytic attack is limited to the outer layer of the implant while the bulk remains virtually unaffected. The size of the implant decreases and its mechanical properties vary with time in a predictable fashion.

Another factor that might play an important role in the hydrolytic degradation of as-pol. PLA100 is its characteristic morphology which results from the melt (bulk) polymerization. Until now the relationship between this morphology and the above-mentioned factors has not been widely studied.

By hot-drawing, a process of orientation at elevated temperatures close to the melting temperature the morphology of PLA100 can be altered drastically to give high strength high modulus fibers, that can be applied as sutures. Generally, when placed under a load that is small compared with its maximum strength a material will show cracking under the influence of a non-solvent medium.

The aim of this paper is to investigate the influence of morphology on the long-term in vitro and in vivo degradation of as-pol. PLA100. In the second part of this paper we would like to present some remarkable results from long-term in vitro degradation of a hot-drawn PLA100 fiber placed under a static load.

Theoretical considerations

Crystallinity, heat of fusion and mass loss

The crystallinity χ_c of a polymeric material is expressed as the ratio of the heat of fusion ΔH_f and that of the pure crystalline material ΔH^0:

$$\chi_c = \Delta H_f / \Delta H^0 \ . \tag{1}$$

Crystalline and amorphous material do not necessarily hydrolyze at an equal rate. At any degradation time t, the mass of crystalline material $m_c(t)$ can be expressed as

$$\begin{aligned} m_c(t) &= \chi_c(t) m(t) = (\Delta H_f(t)/\Delta H^0) m(t) \\ &= (\Delta H_f(t)/\Delta H^0) m_0 (1 - m_l(t)) \ , \end{aligned} \tag{2}$$

where m_0 is the initial mass, $m(t)$ the remaining mass and $m_l(t) = 1 - m_0/m_t$ the mass loss. The amount of crystalline material relative to the initial value $m_{c,0}$ is a function of time:

$$m_c(t)/m_{c,0} = (\Delta H_f(t)/\Delta D_{f,0})(1 - m_l(t)) \tag{3}$$

with $\Delta H_{f,0}$ the heat of fusion of the original material.

A constant $m_c(t)/m_{c,0}$ with time (constant amount of crystalline material $m_c(t)$) indicates that only the amorphous fraction degrades. An increasing $m_c(t)/m_{c,0}$ points to crystallization, but if $m_c(t)/m_{c,0}$ decreases, the crystalline material hydrolyzes.

Presenting ΔH_f- and mass loss data according to Eq. (3) distinguishes between crystallization and preferential solubilization of the amorphous fraction and provides a means to investigate the stability of the crystalline fraction.

Permeation of water

Although poly(lactide)s are generally considered hydrophobic, water is able to permeate these materials causing hydrolytic degradation.

The transport of gases and vapors in polymers can be described by the coefficients of sorption (S) and diffusion (D) and permeability $P = DS$. Sorption and especially diffusion strongly depend on the fractional free volume f, which is much smaller for crystallites than for the amorphous phase. Consequently, in semi-crystalline polymers, sorption and diffusion in the crystalline phase can be neglected and most of the transport takes place in the amorphous phase [19].

The qualitative relationships connecting the fractional free volume f and the crystallinity χ_c of the polymer to the diffusion coefficient D for liquids in polymers ($\sim 10^{-9}$–10^{-6} cm^2/s) are

$$\begin{aligned} D &= D_a(1 - \chi_c) \ , \\ D_a &\sim D_0 \exp(-1/f) \ , \end{aligned} \tag{4}$$

where D_a is the diffusion coefficient of the liquid in the atmorphous polymer.

The equilibrium sorption of water not only depends on fractional free volume f, but is also influenced by the accessibility of polar groups on crystallite surfaces, which may "react" with water. If for a high molecular weight poly(lactide) the influence of hydroxyl- and carboxylic end-groups may be neglected, then for PLA100 ($\chi_c = 0.7$) an equilibrium water sorption of 1.5 wt% can be estimated from group contributions [20], compared to 5 wt% for amorphous poly(lactide). Experimentally, for PLA100 an equilibrium water sorption of 1.8 wt% has been established [12], which compares well with the estimation.

The sorption of small molecules into glassy polymers frequently fails to follow the $t^{1/2}$ kinetics from Fick's second law. Concentration against depth profiles for this non-Fickian, case II diffusion have been studied by Rutherford backscattering spectrometry [21] and show a concentration front that advances into the polymer at constant velocity. In this layer, which is uniformly swollen,

the glass transition temperature T_g is depressed below room temperature.

However, thermal analysis of poly(lactide)s at equilibrium water sorption did not reveal a decrease of T_g and no plasticizing effect of water has been found during mechanical testing of these samples [12]. Therefore, we may presume that non-Fickian case II diffusion does not play a significant role in the water sorption of poly(lactide)s.

Experimental

Synthesis of L-lactide (co)polymers

D- and L-lactide (Purac Biochem BV) were recrystallized from Sodium-dried toluene. Appropriate amounts of monomer and catalyst (stannous octanoate, Sigma Chemical C.) were added to silanized ampoules under N_2-atmosphere [5, 6]. Ring opening polymerization was performed under high vacuum at temperatures of 100–130 °C for 3–7 days, yielding poly(L-lactide) (100L mol%, PLA100) or poly(D, L-lactide) (50L/50D mol%, PLA50) with high molecular weights (5×10^5–2×10^6 g/mol).

Processing

As-pol. PLA100 was machined into disk-shaped samples or tensile specimens for further testing. PLA50 copolymer was purified by precipitation of a 1% (w/v) chloroform solution into a tenfold excess of cold-stirred ethanol. After drying under vacuum, purified PLA50 was compression-molded at 150 °C in a hydraulic press (PHI) in stainless-steel molds of 2–4 mm thickness.

PLA50 samples were pressure-annealed by cooling from 65 °C to room temperature overnight in a pressurized cylinder immersed in a thermostated bath. Pharmaceutical-grade paraffin oil was used as the pressurizing medium at 200 bar.

PLA100 fiber was prepared by solution spinning of a 7% (m/v) solution of high molecular weight PLA100 polymer in chloroform. The dried as-spun fiber, it was hot-drawn at $T_{draw} = 185$ °C to $\lambda = 5.6$ under a nitrogen atmosphere [22].

Characterization

Composition, monomer conversion and purity of as-pol. and precipitated samples were measured with 200 or 300 MHz ^{1}H-NMR (Varian Gemini 200, Varian VXR 300) in $CDCl_3$. Thermal properties were measured with an indium calibrated Perkin-Elmer DSC7. Samples (5–10 mg) were heated at a rate of 10 °C/min over a variable scanning range between 0 and 200 °C. Glass transition temperatures (T_g) were recorded as the midpoint of the ΔC_p step. Thermal properties of the fibers were measured using 1 mg samples in silicone oil. Molecular weights were determined using SEC (Spectra Physics equipped with Polymer Laboratories 5 μm mixed-C columns, Shodek RI-71 refractometer and Viskotek H502 viscosity detector). Filtered (0.45 μm) 1–2 mg/ml solutions in a suitable solvent like chloroform or THF were measured at 25 °C. Monodisperse poly(styrene) standards (Polymer Laboratories) were used for universal calibration.

Viscosity average molecular weights M_v were calculated from the intrinsic viscosity $[\eta]$ of chloroform solutions using the Mark–Houwink constants [5, 6] ($K = 5.45 \times 10^{-4}$, $a = 0.73$). Tensile properties were recorded with an Instron tensile tester at 20 °C. For the fiber a crosshead speed of 10 mm/min was used at gauge length of 10 mm.

SEM-images of cryogenically fractured samples were produced with an ISI-DS-130 electron microscope after drying and gold sputtering. SEM-imaging of PLA100 fiber after degradation was performed with a JEOL JSM 6320F field emission scanning electron microscope, operated at 1 kV, after drying the samples over P_2O_5 overnight.

Hydrolytic degradation

Disk-shaped samples or rectangular tensile specimens were degraded in flasks filled with sterile water or phosphate-buffered saline (pH = 7.4). The flasks were immersed in a water bath thermostated at 37 °C.

At predetermined intervals, samples were withdrawn from the flasks and weighed before and after drying to constant weight under vacuum at 40 °C. Dried degradation samples were subjected to DSC- and SEC-measurements.

Hydrolytic degradation of PLA100 fiber was conducted in water at room temperature under a static load (10% of the breaking strength, which corresponds to a 20 N load).

Results and discussion

As-polymerized PLA100

As-pol. PLA100 was obtained by bulk or melt polymerization of L-lactide monomer under vacuum at 110 °C in high yields (>99%). Since PLA100 has a melting temperature T_m around 190 °C, during melt polymerization at °C simultaneous growth and crystallization of the polymer

chains occurs. This results in a highly crystalline material with a heat of fusion $\Delta H_f = 77$–95 J/g, depending on the catalyst used [23]. Indeed, as-pol. PLA100 contains large lamellar crystallites which can be observed clearly in SEM (Fig. 1A).

Fig. 1 SEM images of the cryogenic fracture surfaces of (A) as-pol. PLA100, (B) poly(L-lactide) polymerized in the presence of 20% (w/v) toluene and (C) as-pol. PLA100 explanted from a goat after 3.2 yr

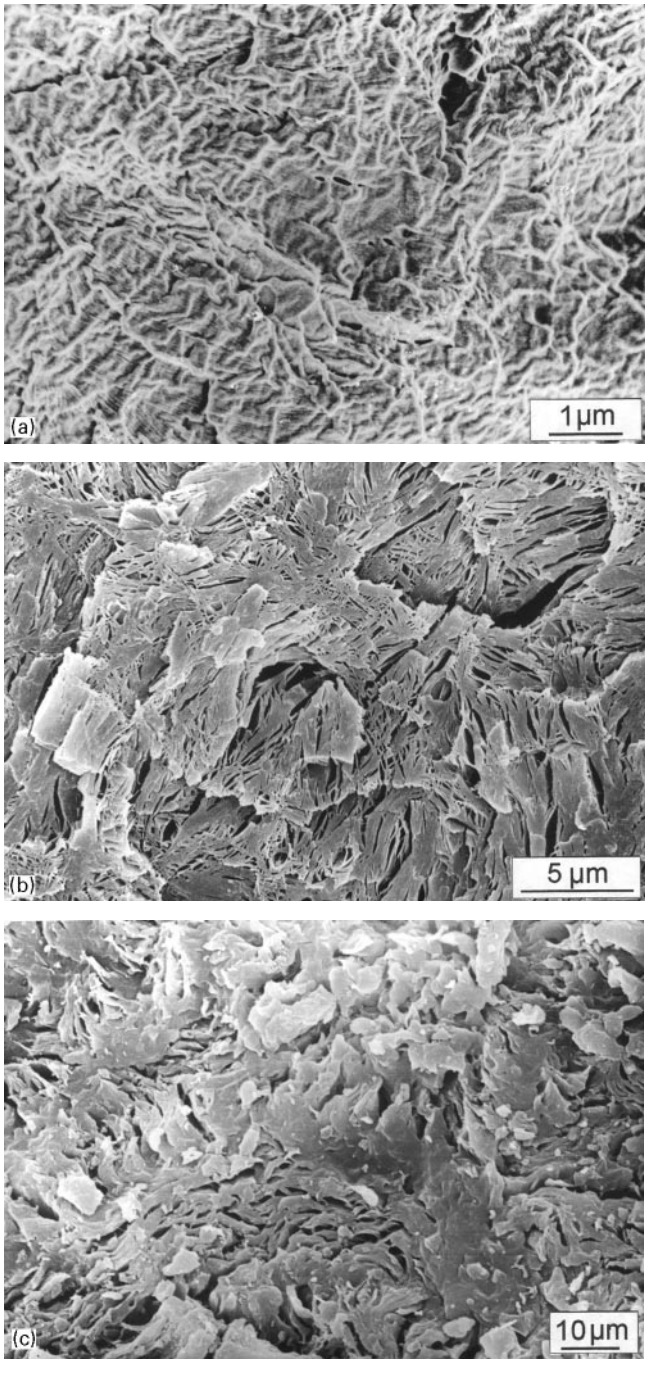

During melt polymerization of PLA100 growing poly (L-lactide) chains crystallize onto adjacent crystallite surfaces. Chain mobility is then limited to free chain ends and repetition of the polymer chains is hindered to a great extent. Therefore, the entanglement density of as-pol. PLA100 will be much lower compared with compression molded PLA100 that has been allowed to cool down from a high temperature ($> T_m$) equilibrium melt [20].

Furthermore, during polymerization shrinkage occurs, because the density of the polymer is higher (~10%) than that of the L-lactide melt. Additional shrinkage (~10%) is caused by crystallization. As a result, substantial thermal stresses develop in as-pol. PLA100 as reflected by the occasional implosion of a polymerization ampoule. These thermal stresses will influence the mechanical properties and degradation behavior of as-pol. PLA100 during application.

To visualize these thermal stresses, L-lactide was polymerized in the presence of 20% (w/v) toluene, which is a good solvent for L-lactide at high temperatures, but does not dissolve poly(L-lactide). In the poly(L-lactide) obtained in the presence of toluene again large lamellar crystallites are present as seen in as-pol. PLA100. However, the fracture surface presented in Fig. 1B shows many fissures, which result from thermal stresses in the material building up during polymerization and cooling down.

A similar pattern of fissures was discovered after an in vivo degradation period of 3.2 yr in the fragile remains of as-pol. PLA100 implanted in goats (Fig. 1C). Mass loss was limited as judged from the presence of a large amount of debris. Also on TEM-images of as-pol. PLA100 explanted after 3 yr, intra- and inter-cellular crystalline debris was clearly visible as lamellae with an average thickness of $d = 22$ nm [14].

Before implantation, as-pol. PLA100 showed $\Delta H_f = 76$ J/g and with SAXS a long period $L = 30$ nm was measured. From these data with $\Delta H^0 =$ J/g [23, 24] the crystallinity $\chi_c = 76\%$ and lamellar thickness $d = \chi_c \times L = 22.8$ nm of as-pol. PLA100 can be calculated. This value agrees well with the lamellar thickness observed with TEM.

After 4 years in vivo the crystallinity of as-pol. PLA100 debris remained appreciably high with $\Delta H_f = 96$ J/g and $T_m = 184\,^{\circ}C$ [14]. Recently, as-pol. PLA100 debris with $T_m = 172\,^{\circ}C$ was explanted from a patient after 8 yr.

From these results it may be concluded that thermal stresses in as-pol. PLA100 lead to disintegration of the implant, but substantial mass loss does not occur, because the remaining crystalline lamellae are little affected by hydrolysis.

The evolution of the tensile properties and molecular weight (MW) during degradation of as-pol. poly(lactide)s

under physiological conditions has been well documented and was shown to depend on the amount of residual monomer [6, 16] and sterilization method [25, 26], which influences the initial MW.

During hydrolytic degradation, the initially high tensile strength of as-pol. PLA100 was lost completely in a period of 11 weeks [6]. This phenomenon can be explained by the low entanglement density and the typical morphology of as-pol. PLA100 described above. Through voids and micro-cracks generated by thermal stresses, water easily penetrates the bulk of the material. Subsequently, chain folds and tie-chains connecting crystallites hydrolyze preferentially, because they are stressed due to a "realing-in" force [24]. Since the amorphous phase contains few entanglements, the material quickly loses its integrity and mechanical properties. Additionally, hydrolysis of chain folds generates hydrophilic groups on the crystallite surfaces, resulting in an increasing osmotic pressure, causing further stress-cracking and facilitation of water penetration. The remaining material mainly consists of large lamellar crystallites which hydrolyze only very slowly.

Further support for this view is found in Fig. 2 which presents a compilation of MW-data vs. degradation time for as-pol. PLA100 during in vivo and in vitro degradation at 37 °C. For the bulk degradation of poly(lactide) copolymers a $\log MW$–t relationship has been derived [27] which takes into account the autocatalytic effect of carboxylic end-groups. Figure 2 shows that initially MW of as-pol. PLA100 decreases faster than that of amorphous PLA50 (dashed curve in Fig. 2), but after 20 weeks the decrease of MW for as-pol. PLA100 slows down, indicating that the remaining material is more stable towards hydrolysis.

A similar transition between two degradation regimes has been observed for a D, L-lactide copolymer containing 2.75 mol% D-lactide during titration degradation with NaOH solution. The MW of the remaining material was shown to be equal to or a multiple of the MW corresponding to the fold-length of the lamellae [28, 29]. Comparable results have been obtained in the degradation of poly (hydroxy butyrate) [30].

To enable extrapolation to $MW \sim 100$ ($MW_{\text{lactoyl unit}} = 72$) the data in Fig. 2 have been replotted on a log–log scale. Figure 3 suggests that total resorption of as-pol. PLA100 takes at least 2000 weaks (40–50 years), which is much longer than anticipated earlier [7–9].

The fate of the crystalline fraction in as-pol. PLA100 can be explored by calculation of $m_c(t)/m_{c,0}$ from ΔH_f-data and mass loss data according to Eq. (3). For the in vivo and in vitro degradation of as-pol. PLA100 the available data are compiled in Fig. 4. Suprisingly, during the first weeks of degradation a small increase of $m_c(t)/m_{c,0}$ is observed, which indicates that some crystallization occurs in as-pol. PLA100. Figure 4 shows similar crystallization for molded PLA100 ($\Delta H_{f,0} = 27$ J/g), which was subjected to accelerated hydrolysis in an alkali medium (0.1 N NaOH) [31].

The crystallization in degrading PLA100 occurs at 37 °C, i.e. below T_g. Similar crystallization has been observed for L-lactide copolymers with D-lactide or glycolide [32]. Apparently, the absorption of water, the decrease

Fig. 2 Molecular weight of poly(lactide)s as a function of degradation time in vivo and in vitro at 37 °C: (●) M_V as-pol. PLA100 [6] and (- - -) M_V PLA50 [27]

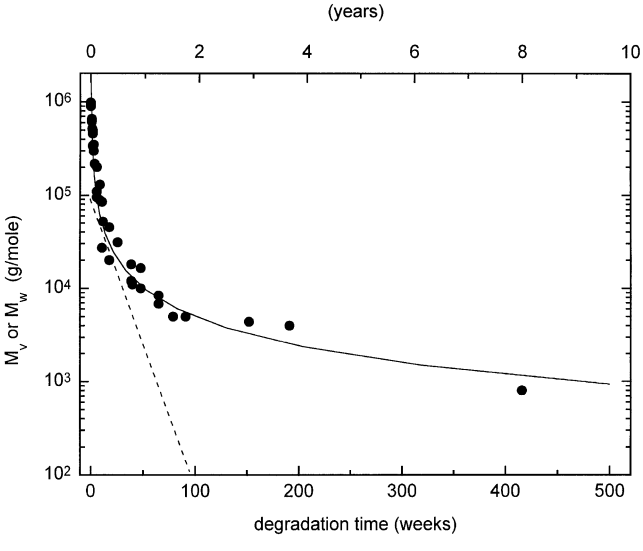

Fig. 3 Molecular weight of poly(lactide)s as a function of degradation time in vivo and in vitro at 37 °C: (●) M_V as-pol. PLA100 [6] and (- - -) M_V PLA50 [27]

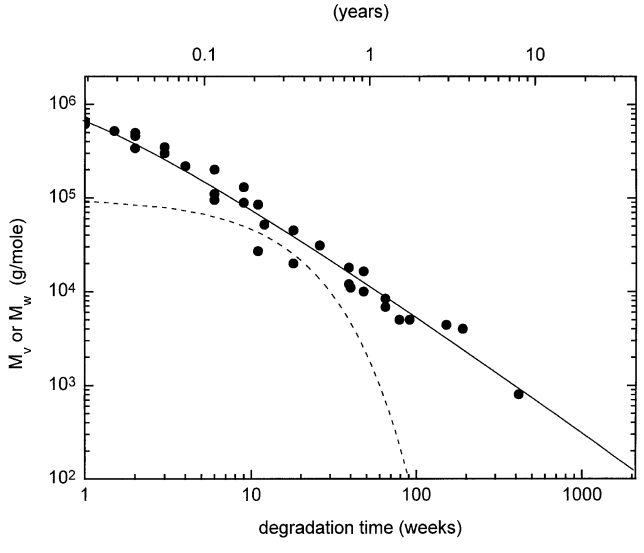

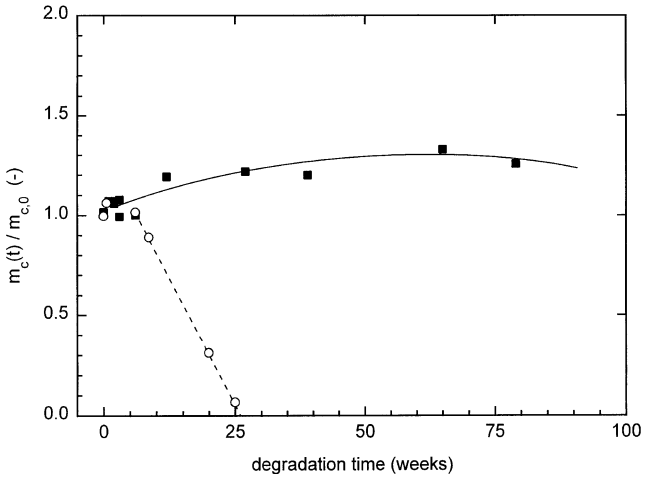

Fig. 4 The relative amount of crystalline material $m_c(t)/m_{c,0}$ as a function of degradation time at 37 °C for: (■) as-pol. PLA100 in vivo and in vitro; (○) moulded PLA100 in 0.1 N NaOH (recalculated from Ref. [27], sample A4)

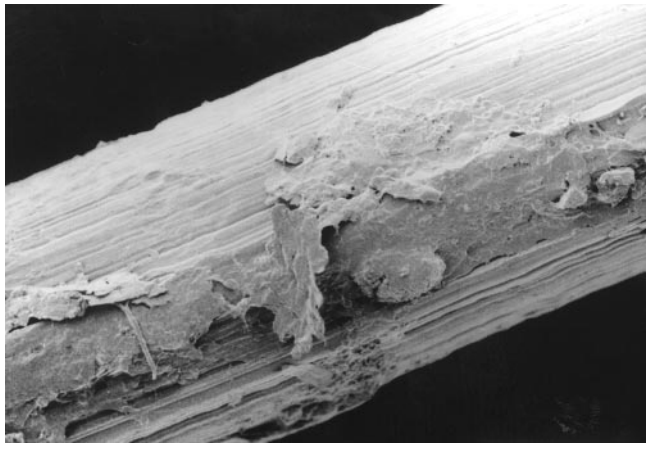

Fig. 5 SEM image of the surface of solution spun hot-drawn PLA100 fibre after hydrolytic degradation under a static load for 5.3 yr at room temperature

of MW by hydrolysis and the resulting decrease of T_g induce an increased mobility of chain fragments, allowing them to crystallize. Furthermore, the large degree of undercooling in the system is a strong driving force for crystallization.

Figure 4 shows that after 70 weeks $m_c(t)/m_{c,0}$ of as-pol. PLA100 tends to decrease, indicating that the crystalline fraction also slowly degrades, probably by etching of the crystallite surfaces. The data for molded semi-crystalline PLA100 ($\Delta H_{f,0} = 27$ J/g) in Fig. 4 suggest that as-pol. PLA100 will also resorb completely after long degradation times, which agrees with the trend observed for MW in Fig. 3. Unfortunately, it is impossible to estimate the in vivo resorption time of as-pol. PLA100 from Fig. 4 by extrapolation of the data to $m_c(t)/m_{c,0} = 0$, because long-term ΔH_f and mass loss data are scarce or non-existent.

Hot-drawn PLA100 fiber

The influence of morphology on the hydrolytic degradation of PLA100 was further investigated in a degradation experiment with solution-spun hot-drawn PLA100 fiber [22]. This fiber was placed in water at room temperature under a static load corresponding to 10% of its maximum strength σ_m.

PLA100 fiber ($\lambda = 5.6$, $\phi = 28.7$ μm) had initial tensile strength $\sigma_m = 750$ MPa. SEM-imaging of the surface of hot-drawn fiber showed few flaws and no micro-pores [33]. The SEM-image in Fig. 5 shows that after immersion in water for 5.3 years the fiber surface is no longer smooth, but no cracks and micro-pores are visible. Rapid failure of the stressed PLA100 fiber was expected due to hydrolysis and stress cracking. In a number of polymers premature failure has been attributed to stress cracking under a static or dynamic load [18, 34]. Surprisingly, for degradation periods up to 64 months (5.3 yr) no break of the fiber was observed. Only a limited reduction of the tensile strength of the fiber was measured from $\sigma_m = 750$ to 590 MPa. After 64 months the diameter of the hot-drawn PLA100 fiber had decreased to $\phi = 25.9$ μm, corresponding to a reduction in diameter of ~10%. Extrapolation to $\phi = 0$ yields an estimation of a total degradation time of 50 yr, which agrees well with the extrapolation for as-pol. PLA100 (40–50 yr, see Fig. 3).

The extreme stability towards hydrolysis and stress cracking of hot-drawn PLA100 fiber can be explained by the morphology obtained after orientation at elevated temperatures. By the hot-drawing process hydrolytically sensitive chain folds have been removed. Furthermore, SAXS analysis [35] has established that micro-voids can be eliminated from solution-spun PLA100 fibers by drawing to an optimum drawing ratio ($\lambda \sim 8$). The high perfection of the fiber combined with its high crystallinity probably results in an very small fractional free volume [19] which renders oriented PLA100 fiber virtually impenetrable to water. Hence, stress-cracking by build-up of osmotic pressure in the bulk which caused fragmentation in as-pol. PLA100 is prevented in oriented PLA100 fiber. Hydrolysis is restricted to crystallite surfaces facing the outside of the fiber, which proceeds at a similar rate as with the lamellar crystallites in debris from as-pol. PLA100.

Contrary to the bulk degradation observed for as-pol. PLA100, the hot-drawn PLA100 fiber now degrades by surface erosion accompanied by a very slow decrease of its diameter and mechanical properties.

General

The exceptional hydrolytic stability of its crystalline phase, indicates that highly crystalline L-lactide compositions are not suitable for use in degradable biomedical devices. Therefore, at the expense of a reduction of stiffness and strength, amorphous lactide-based materials have been developed.

By molding and "orientrusion" [36, 37] of crystallizable poly(lactide) compositions poly(lactide)s with reduced crystallinity have been obtained. However, as indicated earlier in this study, some crystallinity might develop in these quenched materials during degradation. Although no disturbing problems have yet manifested themselves in certain clinical applications [38–41], crystallization may compromise the long-term biocompatability of these materials.

Copolymerization of L-lactide with D-lactide, glycolide, ε-caprolactone and trimethylene carbonate has yielded non-crystallizable materials with a broad spectrum of initial properties and hydrolytic bulk degradation patterns [42–50].

Absorption of water in the bulk could be suppressed if thermal stresses and micro-voids were eliminated, e.g. by annealing under high pressure [51]. Pressure-annealing (200 bar, paraffin oil) of PLA50 resulted in an increased density $\rho = 1.260$ compared with 1.251 for conventionally molded PLA50. Such pressure-annealed, fully enthalpy-relaxed materials, free of voids and residual stresses should possess a low sensitivity towards water-treeing, possibly shifting the degradation pattern from bulk to surface erosion.

During the in vitro degradation of amorphous PLA50 extremely small amounts of crystalline residue have been found, originating from low MW isotactic sequences or generated by stereo-complex formation [52, 53]. It remains to be investigated whether this debris will induce long-term clinical complications.

Conclusions

The results of the present study clearly indicate that the morphology obtained from the melt polymerization of semi-crystalline as-pol. PLA100 has a significant influence on the course of its hydrolytic bulk degradation. The generation of micro-cracks by residual thermal stresses and an increasing osmotic pressure facilitate water absorption and cause a rapid loss of tensile properties and a fast initial decrease of molecular weight.

During degradation at temperatures below T_g crystallization was observed, which may be caused by an increased mobility of the polymer chains due to a decrease in molecular weight and T_g.

After many years a highly crystalline debris remains, which is very stable towards hydrolysis. By extrapolation of molecular weight data the resorption time of as-pol. PLA100 in vivo was estimated at 40–50 yr.

The morphology of poly(L-lactide) could be altered dramatically by hot-drawing of solution-spun fiber. After more than five years the oriented fiber had retained more than 75% of its initial tensile strength, indicating extreme hydrolytic stability. Surprisingly, under a static load no stress-cracking of the fiber was observed. SAXS-analysis suggested that by hot-drawing micro-voids are eliminated, which makes the fiber impenetrable to water. Furthermore, orientation reduces the number of hydrolytically sensitive chain folds. This highly perfect highly crystalline morphology induces the fiber to degrade through surface erosion as indicated by a small decrease of its diameter.

Possibly, orientation or high-pressure annealing could also eliminate voids and thermal stresses from amorphous poly(lactide). It remains to be investigated whether this leads to amorphous poly(lactide) materials which degrade by surface erosion.

In view of the hydrolytic stability of the crystalline residue for application in degradable biomedical devices non-crystallizable L-lactide copolymers are preferred.

References

1. Cutright DE, Hunsuck EE, Beasly JD (1971) J Oral Surg 29:393
2. Kulkarni RK, Moore EG, Hegyeli AF, Leonard F (1971) J Biomed Mater Res 5:169
3. Gilding DK, Reed AM (1979) Polymer 20:1459–1464
4. Reed AM, Gilding DK (1981) Polymer 22:494–498
5. Leenslag JW, Pennings AJ, Bos RRM, Rozema FR, Boering G (1987) Biomaterials 8:70–73
6. Leenslag JW, Pennings AJ, Bos RRM, Rozema FR, Boering G (1987) Biomaterials 8:311–314
7. Bos RRM, Rozema FR, Boering G, Leenslag JW, Verweij AB, Pennings AJ (1989) Dtsch Z Mund Kiefer Gesichts Chir 13:422–424
8. Bos RRM, Rozema FR, Boering G (1991) Biomaterials 12:32–36

9. Bos RRM, Rozema FR, Boering G, Nijenhuis AJ, Pennings AJ, Jansen HWB (1989) Br J Oral Maxillofac Surg 27:467–476
10. Bos RRM, Rozema FR, Boering G, Nijenhuis AJ, Pennings AJ, Verweij AB (1987) J Oral Maxillofac Surg 45: 751–753
11. Rozema FR, Bos RRM, Pennings AJ, Jansen HWB (1990) J Oral Maxillofac Surf 48:1305–1309
12. Grijpma DW, Nijenhuis AJ, van Wijk PGT, Pennings AJ (1992) Polym Bull 29:571–578
13. Rozema FR, Bos RRM, Pennings AJ, Jansen HWB (1994) Cells Mater 4:31–36
14. Rozema FR, de Bruin WC, Bos RRM, Boering G, Nijenhuis AJ, Pennings AJ (1992) In: Doherty PJ, Williams RL, Williams DF, Lee ATL (eds) Biomaterial–Tissue Interfaces, Advances in Biomaterials, Vol 10. p 349
15. Bergsma JE, de Bruin WC, Rozema FR, Bos RRM, Boering G (1995) Biomaterials 16:25–31
16. Nakamura T, Hitomi S, Watanabe S, Shimizu Y, Jamshidi K, Hyon S-H, Ikada Y (1989) J Biomed Mater Res 23:1115–1130
17. Domb A, Ron E, Langer R (1989) In: Mark HF, Bikales NM, Overberger CG, Menges G (eds) Polyanhydrides. Encyclopaedia of Polymer Science and Technology, 2nd ed. Wiley, New York (supplement volume) p 648
18. Daniels AU, Andriano KP, Smutz WP, Chang MKO, Heller J (1994) J Appl Biomater 5:51–64
19. Peterlin A (1975) J Macromol Sci-Phys B 11:57–87
20. van Krevelen DW (1990) Properties of Polymers, 3rd ed. Elsevier, Amsterdam
21. Mills PJ, Kramer EJ (1986) J Mater Sci 21:4151–4156
22. Penning JP, Dijkstra H, Pennings AJ (1993) Polymer 34:942
23. Nijenhuis AJ, Grijpma DW, Pennings AJ (1992) Macromolecules 25:6419
24. Nijenhuis AJ, Grijpma DW, Pennings AJ (1991) Polym Bull 26:71–77
25. Cordewener FW, Rozema FR, Bos RRM, Boering G (1995) J Mater Sci, Mater Med 6:211–217
26. Cordewener FC (1996) PhD thesis, Chapter 6, Groningen
27. Buchholz B (1992) In: Planck H, Dauner M, Renardy M (eds) Degradation Phenomena on Polymeric Biomaterials. Springer, Berlin
28. Fischer EW, Sterzel HJ, Wegner G (1973) Koll Z u Z Polym 251:980–990
29. Fischer EW (1975) Progr Colloid Polym Sci 57:149–163
30. Welland EL, Stejny J, Halter A, Keller A (1989) Polymer Comm 30:302
31. Cam D, Hyon S-H, Ikada Y (1995) Biomaterials 16:833–843
32. Recalculated data from Chu CC (1981) J Appl Polym Sci 26:1727–1734 and Grijpma DW, Nijenhuis AJ, Pennings AJ (1990) Polymer 31:2201–2206
33. Eling B, Gogolewski S, Pennings AJ (1982) Polymer 23:1587
34. Zhurkov SN, Zakrevskyi VA, Korsukov VE, Kuksenko VS (1972) J Pol Sci A-2 10:1509–1520
35. Hoogsteen W, Postema AR, Pennings AJ, ten Brinke G, Zugenmaier P (1990) Macromolecules 23:634
36. Tunc DC (1995) J Biomater Sci, Polym Ed 7:375–380
37. Tunc DC (1985) US Patent 4,539,981
38. Jadhav BS, Tunc DC (1994) In: Gebelein CG, Carraher CE (eds) Biotechnol Bioact Polym [Proc Am Chem Soc Symp] Plenum Press, New York
39. Tunc DC (1986) Polym Prep (Am Chem Soc, Div Polym Chem) 27:431–432
40. Bucholz RW, Henry S, Henley MB (1994) J Bone Joint Surg 76-A:319–324
41. Tunc DC, Jadhav B (1994) Polym Mater Sci Eng 66:411
42. Li S, Garreau H, Vert M (1990) J Mater Sci, Mater Med 1:123–130
43. Li S, Garreau H, Vert M (1990) J Mater Sci, Mater Med 1:131–139
44. Li S, Garreau H, Vert M (1990) J Mater Sci, Mater Med 1:198–206
45. Grijpma DW, Pennings AJ (1993) Macromol Chem Phys 195:1633–1647
46. Grijpma DW, Joziasse CAP, Pennings AJ (1993) Makromol Chem, Rapid Commun 14:155–161
47. Grijpma DW, Pennings AJ (1993) Macromol Chem Phys 195:1649–1663
48. Grijpma DW, van Hofslot RDA, Super H, Nijenhuis AJ, Pennings AJ (1994) Pol Eng Sci 34:1674
49. Joziasse CAP, Topp MDC, Veenstra H, Grijpma DW, Pennings AJ (1994) Polym Bull 33:599
50. Joziasse CAP, Veenstra H, Topp MDC, Grijpma DW, Pennings AJ (1998) Polymer 39:467
51. McKinney JE (1976) Ann New York Ac Sci 279:88–93
52. Li S, Vert M (1994) Macromolecules (Communication) 27:3107–3110
53. Li S, Vert M (1994) Polymer Int 33:37–41